Microphase Boundaries and Chain Conformations in Multiply Branched Diblock Copolymers

Amalie Frischknecht*,†,1 and G. H. Fredrickson‡

Departments of Physics and Chemical Engineering, University of California, Santa Barbara, California 93106

Received March 12, 1999; Revised Manuscript Received July 16, 1999

ABSTRACT: We consider a melt of diblock copolymers consisting of a linear A block connected to a regularly branched B block. A simple "Alexander−de Gennes"-type calculation of the free energy for lamellar, cylindrical, and spherical microphases in strong segregation reveals large shifts in the phase boundaries as a function of the number of generations of the branched block and the functionality of the branch points. Modifying the calculation for the case of just two generations in the branched block, we find that a significant fraction of the second-generation branches fold back to lower the free energy. This is consistent with recent dendrimer theory, which also predicts that branches fold back toward the center. Nevertheless, controlled introduction of branching into copolymer blocks can evidently be quite effective in shifting phase boundaries and thereby influencing mesoscale morphology.

I. Introduction

Block copolymer systems are extremely versatile in that variations of composition, architecture, and choice of monomers can lead to dramatic changes in self-assembly at the mesoscale and, consequently, in properties.[2] For example, commercial materials based on blocks of polystyrene and polybutadiene have properties that vary from high modulus, tough thermoplastics to soft, highly extensible thermoplastic elastomers.[3] To design block copolymers for specific applications it is necessary to have in hand two types of fundamental or empirical knowledge. The first is the relationship between the chemical composition and molecular architecture of the copolymer and its self-assembly behavior. Second, one must establish the relationship between the various copolymer mesophases and the properties that are critical to the application. For example, toughness and high modulus are simultaneously achieved in certain grades of the styrenic block copolymers marketed by Phillips (K-Resins).[4] The high modulus derives from their high styrene content, while toughness can be attributed to their unique mesophase morphology. Phillips utilizes a complex radial architecture to achieve these key properties, which would be difficult or impossible to reproduce with a simple diblock or triblock architecture. The present paper is a contribution to the first body of knowledge—specifically, we explore theoretically the effect of introducing multiple branching into a copolymer block on the location of phase boundaries between lamellar, cylindrical, and spherical mesophases.

Theoretical advances over the past three decades have greatly improved our understanding of the connection between copolymer architecture (and composition) and self-assembly behavior in the melt state. Already in the work of Helfand in the late 1970s,[5] the relationship between block copolymer composition and the thermodynamic stability of the lamellar, cylindrical, and spherical mesophases was firmly established. In the 1980s, Leibler,[6] Semenov[7] and others further developed the analytical machinery to do such calculations. Matsen and Schick's work of the 1990s was a significant advance on the numerical analysis side, which greatly facilitated the exploration of phase diagrams for a variety of new block copolymer architectures and complex mesophases.[8]

Diblock copolymers with similarly shaped monomers and simple interactions (described by a composition-independent Flory χ parameter) are well-known to have a phase diagram that is symmetric in the composition variable ϕ (the volume fraction of the B block). This symmetry can be weakly broken (i.e. phase boundaries shifted) by changing one statistical segment length relative to the other or by switching to a triblock architecture.[9] Calculations for $(AB)_n$ starblock copolymers have also demonstrated modest compositional shifts of phase boundaries for practical values of the number of starblock arms, n.[10]

Much more substantial shifts of phase boundaries were predicted by Milner[11] for A_nB_m copolymers ($n \neq m$), where n A blocks and m B blocks are connected at a central junction point. This includes the important case of a simple A_2B graft (or "Y") copolymer. By forcing unequal numbers of A and B blocks to emerge from the junction points localized at A−B interfaces, the resulting imbalance of chain elasticity in such copolymer melts drives strong interfacial curvature and produces large phase boundary shifts from the symmetric diblock phase diagram. Milner's predictions have been largely confirmed by experimental investigations.[12]

A disadvantage of the A_nB_m architecture is that it is more difficult to synthesize with precise control over arm number (particularly on commercial scales) than the more familiar $(AB)_n$ starblock architecture. An alternative architecture that might also lead to strongly asymmetric phase diagrams would be an AB diblock (or BAB triblock) copolymer with a linear A block and a multiply branched (but flexible) B block(s). Such materials might be prepared in styrenic copolymers by introducing a small amount of a multifunctional monomer into a typical anionic polymerization recipe. Similar architectures involving a *rigid* dendrimer B block and a flexible A block have recently been synthesized,[13] but

† Department of Physics.
‡ Department of Chemical Engineering.

10.1021/ma990372w CCC: $18.00
Published on Web 09/11/1999

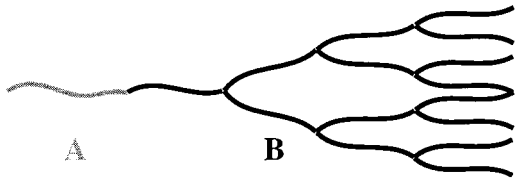

Figure 1. Diblock consisting of a linear A block and regularly branched B block, with $\nu = 4$ generations and $\beta = 2$ branches per branch point.

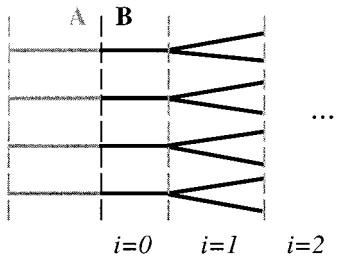

Figure 2. Lamellar phase with step-function profiles. Generations in the branched block are numbered from $i = 0$ to $i = \nu - 1$ (only two generations shown here).

we restrict attention in the present paper to "lightly" branched B blocks that retain considerable conformational freedom.

While a practical implementation of the architecture just described would likely involve *randomly* branched B blocks, we base our theoretical analysis in the present paper on a model of *regularly* branched B blocks depicted in Figure 1. This allows us to estimate the magnitude of phase boundary shifts to be expected in multiply branched block copolymer systems without having to deal with the complexities of the quenched disorder inherent in randomly branched materials. Our analysis is a type of strong segregation theory, which is most accurate for highly incompatible A and B blocks, at low temperature and at high molecular weight. The free energy in such a regime is dominated by chain elasticity and the interfacial energy of A−B monomer contacts across narrow interfaces between microdomains. Under these conditions we expect the chains to be highly stretched away from the AB interface. To calculate the stretching free energy it is convenient to make some assumptions about the chain conformations. The simplest assumption for linear polymers, corresponding to an "Alexander−de Gennes"-type model of the polymer brushes formed by the two blocks,[14,15] is that the distribution of free ends is a delta function at the edge of the brushes (e.g. for the lamellar phase, one assumes that all the free ends lie on the same plane). This approximation leads to an overestimate of the free energy; self-consistent field theories show that instead the free ends are distributed over a layer of finite thickness in the brush, depending on the geometry.[7,16,17] Because of the increasing density in increasing generations of the branched block, the Alexander−de Gennes model for the stretching energy probably leads to a larger error than in the case of linear chains. However, since we are interested in the qualitative effects of the branched block, we will use the simplest possible approximations. We first assume that all the chains stretch radially outward away from the AB interface. For the lamellar phase, we assume that all the branch points in the B block lie on the same plane in each generation, as illustrated in Figure 2, with the free ends of the A blocks also on a single plane. Since we expect

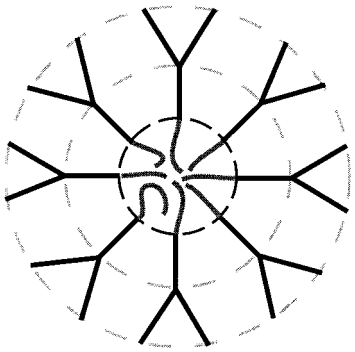

Figure 3. Cylindrical or spherical micelle, with the branch points in each generation lying at the same radial distance from the origin.

that at most volume fractions the branched block would prefer to be on the convex side of interfaces, we calculate only that side of the phase diagram. Thus, for the cylindrical and spherical micelles we take the branch points to all lie on the same shell around the origin in each generation, as shown in Figure 3, but we will use Semenov's[7] self-consistent calculation of the stretching energy for the A blocks in these two cases since clearly not all the A free ends can be at the centers of the micelles.

One can see from Figure 1 that as the number of generations increases, the branched block will pay increasingly large stretching energy costs if all the branches stretch radially away from the A−B interface. A similar problem arises in the case of dendrimers. Recently there has been some controversy in the literature about whether the branches in starburst dendrimers with flexible spacers extend radially outward to the surface or whether some of the branches fold back. An analytical calculation by de Gennes and Hervet[18] implicitly assumed that all the terminal ends were on the outside of the molecule, so that the density was minimal at the core and increased to the outer edge. In contrast, various computer simulations found that the terminal ends were distributed throughout the molecule, implying that some of the branches fold back.[19−21] A recent self-consistent mean field model[22] also found that the chains fold back so that the free ends are distributed throughout the molecule, in agreement with the simulations.

Below we will consider a simple approximation to explore the effects in our block copolymers of branches folding back toward the AB interface. This approximation is a first step toward having a distribution of free ends in the brush, without performing a full-fledged mean-field calculation. We find that, as appears to be the case for dendrimers, the free energy is indeed lower if some of the branches fold back.

II. Theory and Results

We consider diblock copolymers that consist of a linear A block, with degree of polymerization N_A, connected to a branched B block with degree of polymerization N_B, and with $N_A + N_B = N$. The branched block contains ν generations and has β branches per branch point. For generality we take the branches in the ith generation (see Figure 2) to have length N_i, so the fractional degree of polymerization of each branch is $n_i \equiv N_i/N_B$. We must then have

$$\sum_{i=0}^{\nu-1} \beta^i n_i = 1 \tag{1}$$

We use a system of units in which the volume of a monomer is equal to 1, so the volume fraction of the branched blocks is simply $\phi = N_B/N$, and by incompressibility, $N_A/N = 1 - \phi$.

We are interested in how the branched architecture affects the boundaries between the various mesophases. We perform calculations in the strong segregation limit in which the A and B blocks are strongly incompatible, so that the interfaces between A and B are sharp and the copolymers are highly stretched away from the interface. The length scale for a given morphology is determined by the competition between the interfacial energy and the stretching energy of the chains. For the cylindrical and spherical mesophases we calculate the free energy of a cylindrical and spherical micelle, respectively, so that we are assuming that the mesophase has a "round" unit cell. Since cylinders and spheres cannot pack to fill space, this approximation leads to an underestimate of the free energy and consequently to small shifts in the phase diagram.[23,24] In the strong segregation limit these shifts are negligible compared to the effects of the branched block.

First consider the lamellar geometry. Since we are assuming that all the branch points lie on the same plane in each generation, the height of each generation i is determined by the requirement that the chains fill space

$$h_i = \beta^i \sigma N_i \qquad i = 0, 1, \ldots \tag{2}$$

where σ is the number of chains per unit area at the A−B interface and we note that there are β^i branches in the ith generation (also recall that the volume of a monomer is 1). Each branch pays an entropic energy cost for being stretched to the height h_i, $f_i/k_BT = 3h_i^2/2N_ib^2$, where b is the statistical segment length. The stretching energy per B block in units of k_BT is then the sum of the stretching energies of the branches in each generation, summed over all generations:

$$f_B = \sum_{i=0}^{\nu-1} \beta^i \frac{3h_i^{\,2}}{2N_ib^2} = \sum_{i=0}^{\nu-1} \frac{3\beta^{3i}\sigma^2 N_i}{2b^2} \tag{3}$$

Similarly, the stretching energy per chain for the A blocks is simply

$$f_A = \frac{3h_A^{\,2}}{2N_Ab^2} = \frac{3\sigma^2 N_A}{2b^2} \tag{4}$$

where for simplicity we assume the A and B chains have the same statistical segment lengths. In strong segregation the interfacial energy per chain can be written as $f_{int} = \gamma/\sigma$, where γ is the A−B surface tension. The total free energy per chain in terms of the volume fraction ϕ of B and the total degree of polymerization N is then

$$f = \frac{\gamma}{\sigma} + \frac{3\sigma^2 N(1-\phi)}{2b^2} + \sum_{i=0}^{\nu-1} \frac{3\beta^{3i}\sigma^2 n_i N\phi}{2b^2} \tag{5}$$

Minimizing eq 5 with respect to σ, we find that the equilibrium free energy for the lamellar phase is

$$f^*_{lam} = \frac{3}{2}\gamma^{2/3}\left(\frac{3N}{b^2}\right)^{1/3}\left(1 - \phi + \phi\sum_{i=0}^{\nu-1}\beta^{3i}n_i\right)^{1/3} \tag{6}$$

Next consider the cylindrical phase. The chains are no longer uniformly stretched due to the geometry. The volume (per unit length) of the shell bounded by radius r in the ith generation and the radius R_{i-1} of the previous generation must be filled with monomers from the β^i branches, up to the segment n located at r

$$\pi(r^2 - R_{i-1}^{\,2}) = 2\pi R\sigma\beta^i n \tag{7}$$

where R is the radius of the core of the cylindrical micelle, at the A−B interface. Similarly, the number of chains per unit area σ is fixed by the constraint that the A chains in the core of the micelle must fill space, so that $\pi R^2 = 2\pi R\sigma N_A$, which gives $\sigma = R/2N_A$. Differentiating eq 7 gives the rate of stretching per chain, $dr/dn = R\sigma\beta^i/r$, so the stretching energy per B block of the ith layer is

$$\begin{aligned} f_{B,i} &= \frac{3\beta^i}{2b^2}\int_{R_{i-1}}^{R_i} dr\,\frac{dr}{dn} \\ &= \frac{3\beta^i}{2b^2}\int_{R_{i-1}}^{R_i} dr\,\frac{R\sigma\beta^i}{R_{i-1}} = \frac{3R^2\beta^{2i}}{4b^2N_A}\ln\frac{R_i}{R_{i-1}} \end{aligned} \tag{8}$$

where in the final line we have replaced σ with $R/2N_A$. The radius of the ith generation is also given by eq 7

$$R_i^{\,2} = \frac{R^2N_i\beta^i}{N_A} + R_{i-1}^{\,2} \tag{9}$$

with $R_0 = R(N_0/N_A + 1)^{1/2}$ so that

$$R_i = R\left[\sum_{j=0}^{i}\frac{\beta^j n_j\phi}{1-\phi} + 1\right]^{1/2} \tag{10}$$

Substituting into eq 8 and summing over all generations, we find the total free energy of the B block outside the cylinder is

$$f_B = \sum_{i=0}^{\nu-1}\frac{3R^2\beta^{2i}}{4b^2N(1-\phi)}\ln\left[\frac{\left(\phi\sum_{j=0}^{i}\beta^j n_j + 1 - \phi\right)^{1/2}}{\left(\phi\sum_{j=0}^{i-1}\beta^j n_j + 1 - \phi\right)^{1/2}}\right] \tag{11}$$

The free energy of the A blocks in the core of the micelle has been calculated by Semenov,[7] and in our notation is

$$f_A = \frac{\pi^2R^2}{16b^2N(1-\phi)} \tag{12}$$

Finally the surface energy per chain is

$$f_s = \frac{2\pi R\gamma}{2\pi R\sigma} = \frac{2N_A\gamma}{R} \tag{13}$$

Adding the contributions to the total free energy from eqs 11−13 and minimizing with respect to the size of the micelle R, we find that the minimized free energy per chain is

$$f^*_{\rm cyl} = \frac{3}{2}\left(\frac{N(1-\phi)}{b^2}\right)^{1/3} \times (2\gamma)^{2/3}\left[\frac{\pi^2}{8} + \frac{3}{4}\sum_{i=0}^{\nu-1}\beta^{2i}\ln\left(\frac{\phi\sum_{j=0}^{i}\beta^j n_j + 1 - \phi}{\phi\sum_{j=0}^{i-1}\beta^j n_j + 1 - \phi}\right)\right]^{1/3} \quad (14)$$

The calculation for a spherical micelle is very similar to the one above for cylinders. The density constraint for a shell between radius r in the ith generation and the radius R_{i-1} of the previous generation is now

$$\frac{4}{3}\pi\,(r^3 - {R_{i-1}}^3) = 4\pi R^2\sigma\beta^i n \quad (15)$$

Inside the micelle, the incompressibility of the A chains requires that $4\pi R^3/3 = 4\pi R^2\sigma N_{\rm A}$, so that $\sigma = R/3N_{\rm A}$. The stretching energy per B block in the ith layer, using dr/dn from eq 15, is

$$f_{{\rm B},i} = \frac{3\beta^i}{2b^2}\int_{R_{i-1}}^{R_i} {\rm d}r\,\frac{R^2\sigma\beta^i}{r^2} = \frac{R^3\beta^{2i}}{2b^2N_{\rm A}}\left(\frac{1}{R_{i-1}} - \frac{1}{R_i}\right) \quad (16)$$

The radius of the ith generation is now

$$R_i = R\left(\sum_{j=0}^{i}\frac{\beta^j n_j\phi}{1-\phi} + 1\right)^{1/3} \quad (17)$$

so the total stretching energy per chain of the B blocks outside the spherical micelle is

$$f_{\rm B} = \sum_{i=0}^{\nu-1}\frac{R^2\beta^{2i}}{2b^2N(1-\phi)}\left[\frac{1}{\left(\sum_{j=0}^{i-1}\frac{\beta^j n_j\phi}{1-\phi} + 1\right)^{1/3}} - \frac{1}{\left(\sum_{j=0}^{i}\frac{\beta^j n_j\phi}{1-\phi} + 1\right)^{1/3}}\right] \quad (18)$$

From Semenov, the free energy per chain of the A blocks inside the spherical micelle is

$$f_{\rm A} = \frac{3\pi^2R^2}{80b^2N_{\rm A}} \quad (19)$$

and the surface energy per chain is $f_{\rm s} = 3N_{\rm A}\gamma/R$. Minimizing the total free energy $f = f_B + f_A + f_s$ with respect to R gives

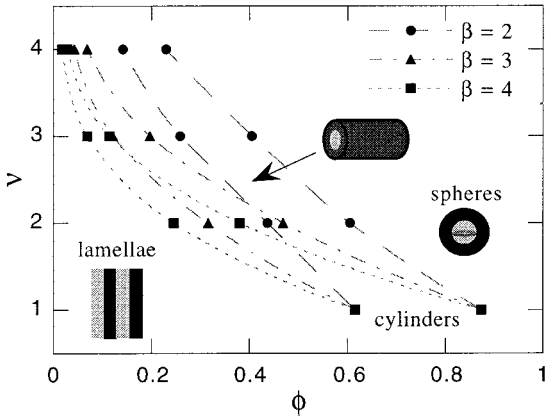

Figure 4. Each pair of symbols at a given generation number ν marks the phase boundaries between the spherical and cylindrical, and the cylindrical and lamellar phases, for different values of the number of branches β per branch point as indicated. Note that the lines are simply guides to the eye.

$$f^*_{\rm sph} = \frac{3}{2}\gamma^{2/3}\left(\frac{9N}{b^2}\right)^{1/3}\left\{\frac{3\pi^2}{40}(1-\phi) + \sum_{i=0}^{\nu-1}\beta^{2i}(1-\phi)^{4/3} \times \left[\frac{1}{\left(\phi\sum_{j=0}^{i-1}\beta^j n_j + 1 - \phi\right)^{1/3}} - \frac{1}{\left(\phi\sum_{j=0}^{i}\beta^j n_j + 1 - \phi\right)^{1/3}}\right]\right\}^{1/3} \quad (20)$$

We can now calculate the phase boundaries between the lamellar, cylindrical, and spherical mesophases from the equilibrium free energies in eqs 6, 14, and 20. So far we have not specified the lengths of the branches n_i in the B block. For illustrative purposes we now take all the branches to have the same length, $n_i = n$, which to satisfy eq 1 means

$$n = \frac{\beta - 1}{\beta^\nu - 1} \quad (21)$$

Figure 4 shows the phase boundaries as a function of the number of generations, ν, for different values of β, the number of branches per branch point. Note that the lines are simply a guide to the eye, since ν can only take on integer values. The results for $\nu = 1$ correspond to linear, diblock copolymers. In this case our free energies for the cylindrical and spherical mesophases are the same as Semenov's,[7] although our lamellar free energy $f^*_{\rm lam}$ for $\nu = 1$ is larger since we assume a step function rather than a parabolic density profile. Thus the phase boundary in Figure 4 between the cylindrical and spherical mesophases for the diblock is the same as Semenov's, but the boundary between the lamellar and cylindrical phases is shifted to $\phi_{\rm lc} = 0.616$ compared with $\phi_{\rm lc} = 0.72$ due to the overestimate of $f^*_{\rm lam}$. In any case we see that the phase boundaries are significantly shifted toward lower volume fractions of B as the number of generations and/or the functionality of the branch points increases.

So far we have assumed that all the branches of the B blocks stretch radially away from the A−B interface. As discussed in the Introduction, one might expect that

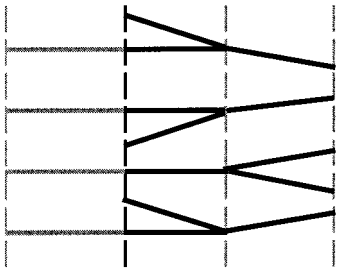

Figure 5. Cartoon of branches folding back toward the A−B interface.

instead some of the branches would fold back toward the interface to lower their stretching energy. For blocks with only two generations, a simple way to incorporate into our calculations the possibility of branches folding back toward the interface is to allow a fraction of the second-generation branches to fold back from the plane of the branch points, as shown for the lamellar case in Figure 5. In the following we assume that all the branches have the same fractional length, n, which for two generations is $n = 1/(1 + \beta)$.

Suppose that a fraction p of the second-generation branches fold back toward the interface, so that there are $1 + p\beta$ branches in the first layer and $(1 - p)\beta$ branches in the second layer. Then for the lamellar geometry, to maintain a constant density the heights of the first and second layers must be

$$h_0 = (1 + p\beta)\sigma N/(1 + \beta)$$
$$h_1 = (1 - p)\beta\sigma N/(1 + \beta) \tag{22}$$

Substituting into eq 3 for the stretching energy of the B block and minimizing with respect to p, we find that the free energy of the branched block is lower when a fraction

$$p = \frac{\beta - 1}{2\beta} \tag{23}$$

fold back. This result is intuitively quite reasonable. For example, for $\beta = 2$, for which we have two branches in the second generation for every chain in the first generation, $p = 1/4$. Since all the branches are the same length, when $p = 1/4$ so that one out of every four second-generation branches folds back, the two layers will have the same height and thus all branches will stretch the same amount; in this case there are three branches in each layer for every two chains.

We can similarly calculate the fraction that fold back for both cylindrical and spherical micelles following the results obtained above previously, although the expressions are more complicated. The stretching energy of the B blocks outside the cylindrical micelle corresponding to eq 11 is

$$f_B = \frac{3R^2(1 + p\beta)^2}{4b^2N(1 - \phi)} \ln(r_0/R) + \frac{3R^2\beta^2(1 - p)^2}{4b^2N(1 - \phi)} \ln(r_1/r_0) \tag{24}$$

while the stretching energy of the B blocks outside the spherical micelle corresponding to eq 18 is

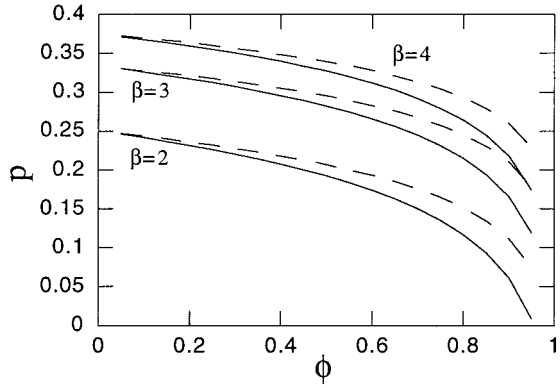

Figure 6. Fraction p as a function of B volume fraction ϕ of branches that fold back in the second generation of the cylindrical (dashed curves) and spherical (solid curves) mesophases, for different functionalities of branch points.

Table 1. Phase Boundaries for $\nu = 2$

	stretched		folded		stars	
	ϕ_{lc}	ϕ_{cs}	ϕ_{lc}	ϕ_{cs}	ϕ_{lc}	ϕ_{cs}
$\beta = 2$	0.437	0.605	0.487	0.722	0.405	0.625
$\beta = 3$	0.315	0.469	0.403	0.612	0.300	0.474
$\beta = 4$	0.245	0.380	0.344	0.474	0.237	0.380

$$f_B = \frac{R^3(1 + p\beta)^2}{2b^2N(1 - \phi)}\left(\frac{1}{R} - \frac{1}{r_0}\right) + \frac{R^3\beta^2(1 - p)^2}{2b^2N(1 - \phi)}\left(\frac{1}{r_0} - \frac{1}{r_1}\right) \tag{25}$$

Here

$$r_0 = R\left(\frac{\phi}{(1 + \beta)(1 - \phi)}(1 + p\beta) + 1\right)^{1/d}$$
$$r_1 = R\left(\frac{\phi}{(1 - \phi)} + 1\right)^{1/d}$$

where $d = 2$ for the cylinders and $d = 3$ for the spheres. Minimizing f_B in each case with respect to p, we find that for both cylinders and spheres p is a function of the volume fraction ϕ and must be found numerically. Figure 6 shows $p(\phi)$ for three values of β. Minimizing the total free energies with respect to R as before then gives the equilibrium free energies with $p(\phi)$ chains folded back from the second generation.

Table 1 shows the phase boundaries for the lamellar to cylindrical, ϕ_{lc}, and cylindrical to spherical, ϕ_{cs}, mesophases of two-generation branched blocks, for stretched blocks (as in Figure 4) and for blocks with folded-back branches. Because the free energy is lower when the chains fold back, the phase diagram is less skewed for this case. The final two columns of Table 1 give the phase boundaries for star polymers with one A leg and β B legs, the architecture discussed by Milner in ref 11. However, for a consistent comparison with our results on the branched architecture we list the phase boundaries for the star polymers as given by an "Alexander−de Gennes" calculation with step-function density profiles, rather than Milner's results, which were for the more accurate parabolic profiles. Clearly a star polymer of this sort is more effective at shifting the phase boundaries toward lower volume fractions of B than is a 2-generation linear-branched block copolymer. Nevertheless, the linear-branched architecture is still fairly effective at shifting the phase boundaries significantly compared to the symmetric diblock phase dia-

gram. Also, even with chains folding back, we would expect the linear-branched block at the third generation to shift the phase boundaries to lower volume fractions than the star polymers.

In summary, our calculations predict the effects on the phase diagram of linear-branched diblock copolymers of adjusting the functionality of the branch points, the number of generations, and the lengths of the branches in each generation. The results are not quantitatively accurate due to the simplifying approximations used, but they could provide a guide toward the design of these sorts of copolymers to produce a desired phase diagram. We also found in a simple way that in a flexible, regularly branched structure, the branches will not stretch radially away from the first generation but instead some will fold back to lower the free energy.

Acknowledgment. This work was supported by the National Science Foundation under Award DMR-9870785. The authors are grateful to Steve Hahn and Scott Milner for helpful discussions.

References and Notes

(1) Present address: Exxon Research and Engineering Co., Annandale, NJ, 08801.
(2) See, for example: Bates, F. S.; Fredrickson, G. H. *Phys. Today* **1999**, *52*, 32.
(3) Holden, G.; Legge, N. R.; Quirk, R. P.; Schroeder, H. E. *Thermoplastic Elastomers*, 2nd ed.; Hanser Publishers: New York, 1996.
(4) Hsieh, H. L.; Quirk, R. P. *Anionic Polymerization*; Marcel Dekker: New York, 1996.
(5) Helfand, E.; Wasserman, Z. R. In *Developments in Block Copolymers*—1; Goodman, I., Ed.; Applied Science: New York, 1982.
(6) Leibler, L. *Macromolecules* **1980**, *13*, 1602.
(7) Semenov, A. N. *Sov. Phys. JETP* **1985**, *61*, 733.
(8) Matsen, M. W.; Schick, M. *Phys. Rev. Lett.* **1994**, *72*, 2660; *Curr. Opin. Colloid Interface Sci.* **1996**, *1*, 329.
(9) Vavasour, J. D.; Whitmore, M. D. *Macromolecules* **1993**, *26*, 7070; Matsen, M. W.; Schick, M. *Macromolecules* **1994**, *27*, 4014.
(10) Matsen, M. W.; Schick, M. *Macromolecules* **1994**, *27*, 6761.
(11) Milner, S. T. *Macromolecules* **1994**, *27*, 2333.
(12) Lee, C.; Gido, S. P.; Poulos, Y.; Hadjichristidis, N.; Tan, N. B.; Trevino, S. F.; Mays, J. W. *J. Chem. Phys.* **1997**, *107*, 6460.
(13) Iyer, J.; Fleming, K.; Hammond, P. *Macromolecules* **1998**, *31*, 8757, and references therein.
(14) Alexander, S. *J. Phys. (Paris)* **1977**, *38*, 983.
(15) de Gennes, P. G. *Macromolecules* **1980**, *13*, 1069.
(16) Milner, S. T.; Witten, T. A.; Cates, M. E. *Europhys. Lett.* **1988**, *5*, 413; *Macromolecules* **1988**, *21*, 2610.
(17) Ball, R. C.; Marko, J. F.; Milner, S. T.; Witten, T. A. *Macromolecules* **1991**, *24*, 693.
(18) de Gennes, P. G.; Hervet, H. *J. Phys. (Paris)* **1983**, *44*, L351.
(19) Lescanec, R. L.; Muthukumar, M. *Macromolecules* **1990**, *23*, 2280.
(20) Mansfield, M. L.; Klushin, L. I. *Macromolecules* **1993**, *26*, 4262.
(21) Murat, M.; Grest, G. S. *Macromolecules* **1996**, *29*, 1278.
(22) Boris, D.; Rubinstein, M. *Macromolecules* **1996**, *29*, 7251.
(23) Matsen, M. W.; Whitmore, M. D. *J. Chem. Phys.* **1996**, *105*, 9698.
(24) Matsen, M. W.; Bates, F. S. *Macromolecules* **1996**, *29*, 1091.

MA990372W